Article

Spin-Orbit Torque from the Introduction of Cu Interlayers in Pt/Cu/Co/Pt Nanolayered Structures for Spintronic Devices

Alberto Anadón,* Rubén Guerrero, Jorge Alberto Jover-Galtier, Adrián Gudín,
Jose Manuel Díez Toledano, Pablo Olleros-Rodríguez, Rodolfo Miranda, Julio Camarero,
and Paolo Perna*

Cite This: https://dx.doi.org/10.1021/acsanm.0c02808

Read Online

ACCESS | Metrics & More | Article Recommendations | Supporting Information

ABSTRACT: Spin currents can modify the magnetic state of ferromagnetic ultrathin films through spin-orbit torque. They may be generated by means of spin-orbit interactions by either bulk or interfacial phenomena. Electrical transport measurements reveal a 6-fold increase of the spin-orbit torque accompanied by a drastic reduction of the spin Hall magnetoresistance upon the introduction of an ultrathin Cu interlayer in a Pt/Cu/Co/Pt structure with perpendicular magnetic anisotropy. We analyze the dependence of the spin Hall magnetoresistance with the thickness of the interlayer, ranging from 0.5 to 15 nm, in the frame of a drift diffusion model that provides information on the expected spin currents and spin accumulations in the system. The results demonstrate that the major responsibility of both effects is spin memory loss at the interface. The enhancement of the spin-orbit torque when introducing an interlayer opens the possibility to design more efficient spintronic devices based on materials that are cheap and abundant such as copper. More specifically, spin-orbit torque magnetic random access memories and spin logic devices could benefit from the spin-orbit torque enhancement and cheaper material usage presented in this study.

KEYWORDS: spin-orbit coupling, magnetic multilayers, materials science, nanostructured devices, interfaces
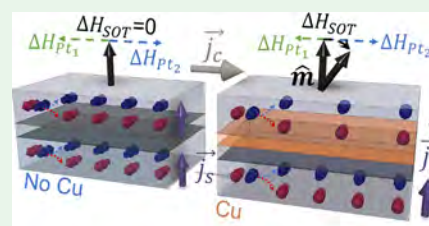
1. INTRODUCTION

The latest advances in spintronics are based on nanometric thin film structures with perpendicular magnetic anisotropy[1−4] in which the spin currents are used to produce changes in the magnetization of a magnetic layer.[5−8] This effect is known as spin-orbit torque (SOT) and can be enhanced by suitably engineering multilayer stacks composed by alternated magnetic/nonmagnetic metals.[8−14] The typical structures employed to manipulate the magnetization via SOT are multilayers whose basic constituent is a ferromagnetic (FM) layer adjacent to heavy metal(s) (HM), which confer large spin-orbit coupling and promote the perpendicular magnetic anisotropy. These systems are the basic elements for spin-orbit torque magnetization switching, used in the next generation of magnetoresistive random access memory (MRAM) devices.[15−18]

The spin-orbit coupling is responsible for bulk phenomena such as the spin Hall effect, the conversion of an electric current into a transverse pure spin current, and its counterpart, the inverse spin Hall effect. At interfaces, where the structural inversion symmetry is broken, interfacial spin orbit interactions are expected to play a critical role in controlling the electronic states as well as the magnetization configurations.[3] The lack of inversion symmetry, proximity effects, orbital hybridization, charge/spin dependent transport, etc. make interfaces between different materials a unique playground environment for the observation of novel physical phenomena.

In presence of a spin current traveling through an interface,[20−22] both bulk and interfacial spin-orbit interactions contribute to the SOT. For instance, a sizable spin-Hall effect has been observed in materials with negligible intrinsic spin-orbit coupling (like Cu, due to the orbital spin-Hall or even insulating oxides),[23,24] revealing the relevance of the interfacial effects.

At the interfaces, interfacial spin-orbit scattering generated by a Rashba spin-orbit field[21] may produce spin precession, spin filtering, and spin memory loss[19,25,26] (schematically illustrated in Figure 1) that have the effect to unbalance the spin accumulation and to produce a torque on the magnetization of an adjacent FM layer. However, the microscopic mechanisms that drive the current-induced magnetization dynamics are still controversial. In fact, the first in-plane current induced magnetization switching in a FM was attributed initially to an interfacial effect (Rashba-induced spin-orbit interaction)[27] while later it was argued to be induced by a bulk spin-Hall effect.[28]
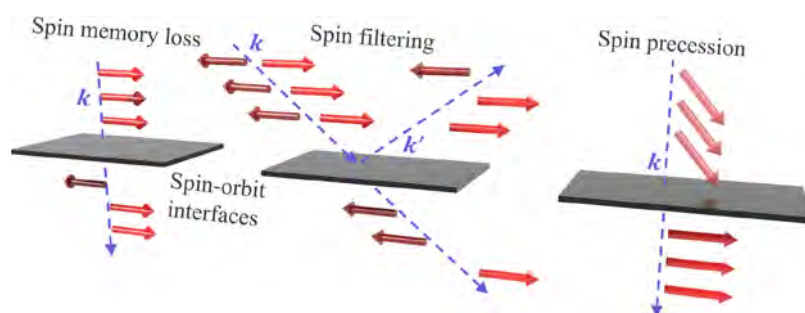
Figure 1. Schematics of spin currents associated phenomena at interfaces with spin-orbit interaction. Spin memory loss is a decoherence process that leads to a reduction of the spin polarization when a spin current passes through an interface. Spin-orbit filtering happens due to carriers with spins parallel and antiparallel to the interfacial spin-orbit field experiencing different scattering amplitudes. When this occurs, reflected and transmitted carriers are spin polarized even if incoming carriers are unpolarized. Spin precession originates from the interaction of electrons with the interfacial spin-orbit field while they traverse the interface and then scatter off.[19] These phenomena arise due to interfacial spin-orbit scattering produced by an interfacial Rashba spin-orbit field and can generate spin-orbit torques.
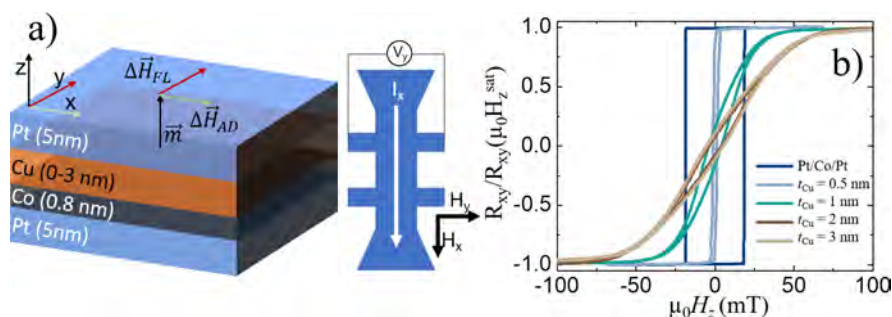

Figure 2. Sample and spin-orbit torque device schematics. (a) Schematic illustration of the structure and the Hall bar device for SOT measurements. (b) Normalized room temperature transversal resistance as a function of the out of plane field for the structures with a different Cu thickness interlayer. The increase of the thickness of the Cu interlayer produces a decrease in the effective perpendicular magnetic anisotropy.

To separate bulk and interfacial contributions, asymmetric interfaces, in which the FM layer is embedded between two different nonmagnetic (NM) or HM materials, all a few nanometers thick, can be used to unbalance the spin-orbit interactions originated at the two interfaces. Recently, an enhancement of the spin-orbit torque has been observed in interfacial spin scattering experiments by introducing sub-monolayer thick metal interlayers inside the HM[22] or by underlying 2D materials such as MoS_2.[29] In similar asymmetric systems, a new purely interfacial magnetoresistance effect, named spin-orbit magnetoresistance ascribed to Rashba spin-orbit interaction, has been predicted[30] and observed in ultrathin Cu-capped Pt/YIG systems producing an increase of the magnetoresistance.[31] Moreover, ab initio studies predicted that in-plane charge currents in Co/Pt and Pt/Cu interfaces can produce spin currents as large as those generated by spin-Hall in bulk Pt.[19−21] Therefore, a more thorough experimental analysis of the interfacial effects is needed to understand the underlying phenomena and potentially obtain more efficient SOT devices. To this aim, Cu is a particularly promising material for applications given its low spin-orbit interaction and its bulk long spin diffusion (λ_{sd}).

In this work, we demonstrate experimentally a substantial increase of the SOT efficiency when introducing a nanometric Cu interlayer in a Pt/Cu(t_{Cu})/Co/Pt stack, which is promising for spintronic devices such as as MRAM based on spin-orbit torque and spin logic devices. The enhancement of SOT that we find cannot be explained by the bulk spin-Hall effect given the negligible spin-Hall angle of Cu and considering the long spin diffusion in Cu, which can be as large as hundreds of

nanometers[32,33] making the Cu spacer between Pt and Co almost transparent to the spin currents generated by the spin-Hall effect in Pt but can be solely ascribed to interfacial effects. The combined torques and spin magnetoresistance experiments as a function of the Cu interlayer thickness demonstrate that spin currents generated at the interfaces are transduced directly to SOT. The magnitude of this effect must be proportional to the spin current density and independent of its polarization, so that our observation of a diminished spin magnetoresistance proves that spin memory loss drives the enhancement of the SOT. A simple drift diffusion model, based on the Valet−Fert model,[34] which accounts for spin currents and spin accumulation at the Cu/Co interface, reproduces satisfactorily the behavior of the spin magneto-resistance for small and large Cu thickness when the spin memory loss is introduced.

2. METHODS

The samples were prepared by DC sputtering onto thermally oxidized (300 nm) silicon substrates at Ar partial pressure of 8×10^{-3} mbar. The base pressure of the chamber was 10^{-8} mbar. The film thicknesses were monitored in situ using a quartz microbalance and confirmed by X-ray reflectivity experiments. The samples consisted in the following stack: Pt(5 nm)/Cu(t_{Cu})/Co(0.8 nm)/Pt(5 nm)/Ta(5 nm)//SiO$_2$(300 nm)/Si, with t_{Cu} ranging from 0 to 3 nm. For t_{Cu} = 0 nm (reference sample), we used a thicker Pt bottom layer to promote a net spin current that yields to a measurable SOT. For spin-Hall magnetoresistance measurements, we use a t_{Cu} up to 15 nm.

The samples were processed using optical lithography to define Hall bar devices with a channel width of 15 μm (photoresist AZ1512 and Ar milling etching were used). Ta(10 nm)/Cu(100 nm)/Pt(10

nm) electrical contacts were defined in a second optical lithography by DC sputtering.

Spin-orbit torque experiments were performed at room temperature as a function of a constant in-plane magnetic field, applied either along the $\hat{\mathbf{x}}$ or $\hat{\mathbf{y}}$ directions, as shown in Figure 2a. This technique, detailed in refs 35−37, allows for the estimation of antidamping-like (AD) and field-like (FL) torques induced to the FM. The torques are measured by analyzing the first and second harmonic voltage response to a periodic electric current signal applied in the $\hat{\mathbf{x}}$ direction. The effective AD and FL torques ($\chi_{AD,FL}$) are obtained using the following equation:

$$\chi_{AD,FL} = -2 \frac{\partial V^{2\omega}}{\partial H_{X,Y}} \Big/ \frac{\partial^2 V^{\omega}}{\partial H_{X,Y}^2} \tag{1}$$

The contribution from the planar Hall effect is then considered and subtracted from the measured values of the effective SOT.[38] See the Supporting Information for more details. The field dependent magnetization reversal pathways of the stacks were studied by means of Kerr magnetometry and the anomalous Hall effect. The inclusion of the Cu interlayer gave rise to a reduction of the remanence magnetization, as shown in Figure 2b, similarly to what was observed by Okabayashi et al.[39] Spin-Hall magnetoresistance (SMR) measurements were finally carried out at room temperature using a 1 T magnetic field and up to 5 mA in plane current. The sample was rotated in the xy, xz, and yz planes using a stepper motor.

Finally we have developed a drift-diffusion model based on Valet−Fert[34] to account for the spin currents and spin accumulation in the system in order to further investigate the SMR dependence with t_{Cu}. Details of the model can be found in the Supporting Information.

3. RESULTS AND DISCUSSION

3.1. Spin-Orbit Torques in Pt/Co/Pt and Pt/Cu/Co/Pt.

We measured the antidamping-like (χ_{AD}) and field-like (χ_{FL}) torques as a function of the thickness of a Cu interlayer (t_{Cu}) ranging from 0 to 3 nm in the Pt(5)/Cu(t_{Cu})/Co(0.8)/Pt(5) stack (Figure 3). In the case of absence of the Cu interlayer
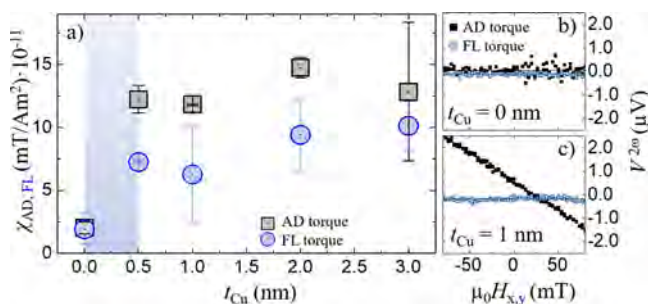

Figure 3. Spin-orbit torque in Pt/Co/Cu(t_{Cu})/Pt stacks, as a function of the Cu thickness t_{Cu}. Antidamping-like torque increases 6-fold when the Cu interlayer is introduced while field-like torque increases by a factor of 3. (a) Evolution of the antidamping-like and field-like torques with t_{Cu}. (b) Antidamping-like and field-like torques for the sample without a Cu interlayer and (c) for t_{Cu} = 1 nm. $\chi_{AD,FL}$ are calculated as shown in eq 1 and then the contribution from the planar Hall effect is subtracted (see refs 36 and 38).

(t_{Cu} = 0) we observe minimal values for both χ_{AD} and χ_{FL}, as expected since the spin currents on top and bottom interfaces with Co are compensated (the direction of the spins point against each other due to the symmetry of the spin Hall effect), and therefore the observed SOT in both directions is small, i.e., $\chi_{AD,FL} < 2 \times 10^{-11}$ mT/A m². Once a Cu interlayer is introduced (t_{Cu} = 0.5 nm), we observe a 6-fold increase of the antidamping-like torque up to $\chi_{AD} = 12 \pm 2 \times 10^{-11}$ mT/A m², whereas χ_{FL} increases by a factor of 3. This value of χ_{AD} is

comparable to the ones obtained in TaO$_x$/Co/Pt[37,38] or AlO$_x$/Co/Pt trilayers[40,41] in which the spin-Hall effect in Pt is the main contribution.

As the Cu interlayer thickness is further increased, χ_{AD} and χ_{FL} do not vary significantly, and the latter remains smaller than χ_{AD} in the whole thickness range. This behavior suggests that the effect arises due to the inclusion of the Co/Cu interface and not due to spin accumulation changes nor to spin-orbit interaction induced by proximity in the Cu layer. Moreover, since for large Cu thickness, both χ_{FL} and χ_{AD} are substantially unmodified, the observed enhancement of SOT at small thickness cannot be related with the Cu layer itself but it is rather due to a purely interfacial effect. This may be caused either by the generation of spin currents at both Cu interfaces via spin filtering and spin precession mechanisms or due to a loss of spin current polarization by means of spin memory loss. However, spin memory loss or interfacially generated spin currents cannot be distinguished by SOT measurements alone. Spin-Hall magnetoresistance experiments provide the means to discern about the origin of this enhancement. In the case of spin memory loss, a decrease in the SMR is expected, while this is not the case for the interfacially generated spin currents, as discussed in the following section.

3.2. Spin-Hall magnetoresistance in Pt/Co/Pt and Pt/Cu/Co/Pt.

SMR is the change of resistance in a FM/HM bilayer depending on the relative orientation of **m** (reduced magnetization $m = M/M_{sat}$) and $\mathbf{j_c}$ (charge current density) vectors.[42−44] This phenomenon is an effect of the spin current density generated in the HM impinging in the FM and being adsorbed by it, thus generating a second spin current in the HM that by the inverse spin-Hall effect is converted into an extra voltage.[43] As the absorption depends on the FM magnetization direction and the spin current generated in this experiment is oriented along the $\hat{\mathbf{y}}$ direction, the SMR is expected to be maximum when the magnetization of FM is parallel to $\hat{\mathbf{y}}$. The magnitude of the SMR is proportional to the squared spin-Hall angle of the HM (θ_{SH}, the efficiency of the spin current−voltage conversion) and to the spin mixing conductance.

In the following, we analyze the Cu thickness behavior of the SMR and anisotropic magnetoresistance. The geometry of the measurements is shown in Figure 4a. The rotation in the xy plane combines anisotropic magnetoresistance and SMR, while the rotation in the zx and zy planes yield to the anisotropic magnetoresistance and SMR signals, respectively. The dependence of the device resistance on the orientation of the magnetic field in the xy, xz, and zy planes is shown in panel b of Figure 4.

A sizable magnetoresistance appears in the three planes, and the observed magnitude is in agreement with previous studies.[6] The magnitude of the SMR is given by the ratio of the resistance difference between the maximum and minimum values and the minimum resistance (SMR = $(\Delta R/R)^{yz\ plane}$ = $(R_{max} - R_{min})/R_{min}$) upon rotation of the magnetic field in the yz plane. The evolution of this magnitude with t_{Cu} is shown in Figure 4c. The plots in panels b and c show that the SMR magnitude decreases upon the introduction of the Cu layer and then slightly increases for larger thicknesses. Such a reduction of SMR is compatible with a reduction of the average spin current in the system, as a result of an enhancement of the spin memory loss. The generation of spin currents would produce an enhancement of the spin accumulation at interfaces and therefore a small increment of the SMR. This has been
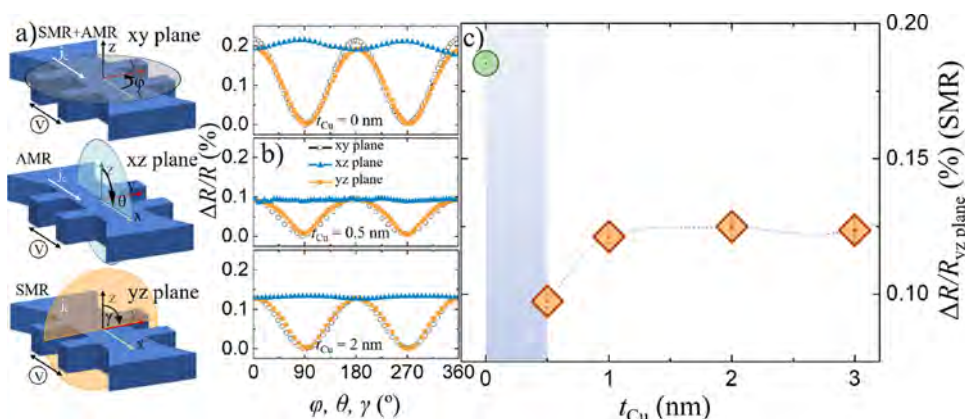
Figure 4. Dependence of the spin-Hall magnetoresistance with Cu thickness. (a) Geometry of the measurement configurations. Spin-Hall magnetoresistance arises in the xy and yz plane configurations, while anisotropic magnetoresistance can be seen in the xz and xy plane configurations. The spin-Hall magnetoresistance signal is observed in the yz plane. (b) Resistance dependence on φ, θ, and γ angles at a magnetic field strength of $\mu_0 H = 1$ T. (c) Evolution of $\Delta R/R$ (spin-Hall magnetoresistance) in the yz plane as a function of t_{Cu}. ΔR represents the resistance difference between the maximum and minimum in the angular dependence, and R is the minimum resistance. The line is a guide to the eye.
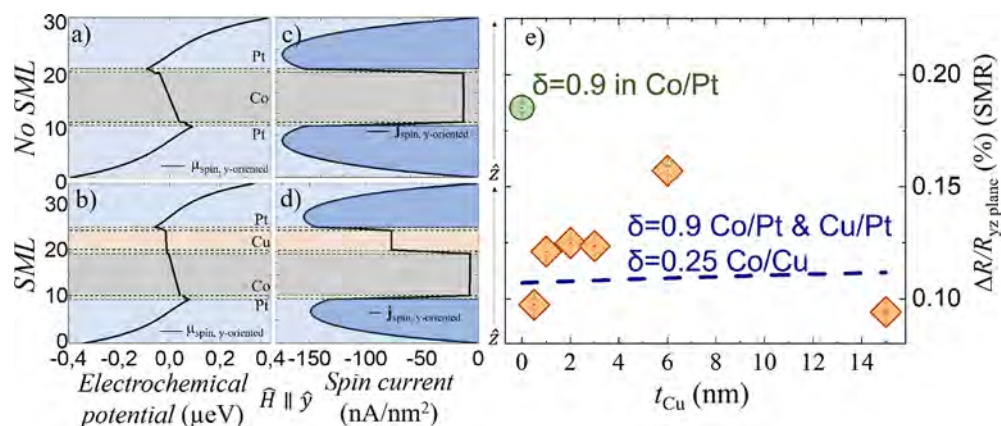

Figure 5. Spin accumulation and spin-Hall magnetoresistance. (a) Calculated spin electrochemical potentials in the system for $\mu_0 H_y = 1$ T, $t_{Cu} = 5$ nm, $t_{Co} = 10$ nm, and $t_{Pt} = 10$ nm considering only spin memory loss in Co/Pt ($\delta_{Co/Pt} = 0.9$) and (b) spin memory loss in all the interfaces (spin flip parameter $\delta_{Co/Pt} = \delta_{Cu/Pt} = 0.9$ and $\delta_{Co/Cu} = 0.25$)[25] with **H** in the $\hat{y}$ direction as well as (c and d) their respective spin currents. Note the decrease of the spin current when spin memory loss is considered. (e) Spin-Hall magnetoresistance as a function of t_{Cu} up to 15 nm. Dashed lines represent the modeled values of SMR as a function of t_{Cu} normalizing the curve at the experimental value of $t_{Cu} = 0$ nm. The calculated SMR values are obtained by taking the difference of the electrochemical potential (spin accumulation) at the edges of the Pt layers (see the Supporting Information). The modeled spin-Hall magnetoresistance decreases linearly as t_{Cu} increases due to the current shunting through Cu. The blue shadowed area in parts c and d represents the spin current that contributes to the total spin-Hall magnetoresistance, which is smaller in the system with spin memory loss.

observed experimentally when adding a thin W layer on top of a YIG/Pt system, even though W has the opposite sign of the spin Hall angle when compared with Pt.[45] We observe a decrease of the SMR of about 50% when the Cu interlayer is placed. At larger t_{Cu}, SMR slightly increases and then remains approximately constant.

This decrease in SMR when introducing the Cu interlayer suggests that the main mechanism involved in this behavior is spin memory loss. To further understand the evolution of SMR and SOT with t_{Cu}, we have developed a drift-diffusion model to obtain the spin currents and accumulations in the system. This model is detailed in the Supporting Information. Figures 5a,b and 5c,d show, respectively, the $\hat{y}$-oriented spin accumulations and the out of plane $\hat{y}$-oriented spin current densities for an external magnetic field along the $\hat{y}$ direction (with the Cu interlayer). The SMR depends on the average spin current densities of both upper and bottom Pt layers (see the Supporting Information), which gives rise to the spin-Hall

voltage via inverse spin-Hall effect. In order to further analyze the behavior of SMR with t_{Cu}, we have extended its range up to 15 nm. These additional samples do not present perpendicular magnetic anisotropy and thus were not considered in SOT measurements.

The SMR extracted from the model (blue dashed line in Figure 5e) slightly increases when t_{Cu} increases. The spin memory loss reduces the spin current that flows through the Co/Cu interface (see Figure 5c,d). For this calculation, we use a depolarization probability of 60% for Pt/Cu and Pt/Cu interfaces and 22% for the Co/Cu interface,[25,26] which corresponds to a spin-flip parameter δ of 0.9 and 0.25, respectively (see the Supporting Information). Figure 5e shows that when the spin memory loss is accounted for, the total SMR decreases 43%. This behavior mimics the decreasing trend of our experimental observation when comparing both the Pt/Co/Pt and the Pt/Cu/Co/Pt samples. Here, spin memory loss is mainly responsible for the observed decrease in

SMR since both positive and negative spin currents would lead to a higher total SMR (as it is proportional to the squared spin-Hall angle and its magnitude does not depend on the spin current sign). This indicates that the SMR reduction is due to spin memory loss and is compatible with the both high and low t_{Cu} regimes. At intermediate t_{Cu}, other additional effects must be also considered to describe completely the evolution of SMR with t_{Cu}. It is worth noting that although spin memory loss is typically considered to be a drawback in spintronic devices due to the detrimental overall magnetoresistance output, the accumulation of unpolarized spins at an interface may be used as a sink of spins to reinject in the device and augment the SOT efficiency.

4. CONCLUSIONS

Spin-orbit interactions can arise in materials at the nanometric scale or at interfaces in which the low dimensionality breaks the structural inversion of symmetry. We have observed the emergence of an interfacially enabled increase of the spin-orbit torque when a Cu interlayer is inserted between Co and Pt in a symmetric Pt/Co/Pt trilayer, in which the effective spin-orbit torque is expected to vanish. The enhancement of SOT is accompanied by a reduction of the spin-Hall magneto-resistance. We infer that spin memory loss in the Co/Cu and Cu/Pt interfaces is mainly responsible for both enhanced SOT and reduction in the SMR at low and high Cu thickness regimes. To understand the behavior at intermediate Cu thicknesses, we highlight the necessity to introduce other interfacial phenomena. The observed enhancement of the spin-orbit torque provides new insight into the interfacial nature of spin currents that can lead to develop more efficient spintronic devices for MRAM spin-orbit torque memories and spin logic using cheap, easy to fabricate, and abundant materials like Cu.

ASSOCIATED CONTENT

Ⓢ Supporting Information

The Supporting Information is available free of charge at https://pubs.acs.org/doi/10.1021/acsanm.0c02808.

> Additional details on the drift diffusion model and on the spin-orbit torque measurements (PDF)

AUTHOR INFORMATION

Corresponding Authors

Alberto Anadón − *IMDEA Nanociencia, 28049 Madrid, Spain;* ⓘ orcid.org/0000-0001-5939-6415; Email: alberto.anadon@imdea.org

Paolo Perna − *IMDEA Nanociencia, 28049 Madrid, Spain;* ⓘ orcid.org/0000-0001-8537-4834; Email: paolo.perna@imdea.org

Authors

Rubén Guerrero − *IMDEA Nanociencia, 28049 Madrid, Spain*

Jorge Alberto Jover-Galtier − *Centro Universitario de la Defensa de Zaragoza, Academia General Militar, 50090 Zaragoza, Spain; Instituto de Biocomputación y Física de Sistemas Complejos and Departamento de Física Teórica, Universidad de Zaragoza, 50009 Zaragoza, Spain;* ⓘ orcid.org/0000-0001-9868-9368

Adrián Gudín − *IMDEA Nanociencia, 28049 Madrid, Spain*

Jose Manuel Díez Toledano − *IMDEA Nanociencia, 28049 Madrid, Spain; Departamento de Física de la Materia Condensada, Departamento de Física Aplicada, and Instituto Nicolás Cabrera, Universidad Autónoma de Madrid, 28049 Madrid, Spain*

Pablo Olleros-Rodríguez − *IMDEA Nanociencia, 28049 Madrid, Spain*

Rodolfo Miranda − *IMDEA Nanociencia, 28049 Madrid, Spain; Departamento de Física de la Materia Condensada, Departamento de Física Aplicada, and Instituto Nicolás Cabrera and IFIMAC, Universidad Autónoma de Madrid, 28049 Madrid, Spain*

Julio Camarero − *IMDEA Nanociencia, 28049 Madrid, Spain; Departamento de Física de la Materia Condensada, Departamento de Física Aplicada, and Instituto Nicolás Cabrera and IFIMAC, Universidad Autónoma de Madrid, 28049 Madrid, Spain*

Complete contact information is available at:
https://pubs.acs.org/10.1021/acsanm.0c02808

Notes

The authors declare no competing financial interest.

ACKNOWLEDGMENTS

REFERENCES

(1) Mangin, S.; Ravelosona, D.; Katine, J. A.; Fullerton, E. E. Current-induced magnetization reversal in nanopillars with perpendicular anisotropy. In *INTERMAG 2006 - IEEE International Magnetics Conference*, San Diego, CA, 2006; 5-5,.

(2) Ikeda, S.; Miura, K.; Yamamoto, H.; Mizunuma, K.; Gan, H. D.; Endo, M.; Kanai, S.; Hayakawa, J.; Matsukura, F.; Ohno, H. A perpendicular-anisotropy CoFeB-MgO magnetic tunnel junction. *Nat. Mater.* **2010**, *9*, 721−724.

(3) Baek, S. H. C.; Amin, V. P.; Oh, Y. W.; Go, G.; Lee, S. J.; Lee, G. H.; Kim, K. J.; Stiles, M. D.; Park, B. G.; Lee, K. J. Spin currents and spin-orbit torques in ferromagnetic trilayers. *Nat. Mater.* **2018**, *17*, 509−513.

(4) Ajejas, F.; Gudín, A.; Guerrero, R.; Anadón Barcelona, A.; Diez, J. M.; de Melo Costa, L.; Olleros, P.; Niño, M. A.; Pizzini, S.; Vogel, J.; et al. Unraveling Dzyaloshinskii−Moriya interaction and chiral nature of graphene/cobalt interface. *Nano Lett.* **2018**, *18*, 5364−5372.

(5) Mihai Miron, I.; Gaudin, G.; Auffret, S.; Rodmacq, B.; Schuhl, A.; Pizzini, S.; Vogel, J.; Gambardella, P. Current-driven spin torque induced by the Rashba effect in a ferromagnetic metal layer. *Nat. Mater.* **2010**, *9*, 230−234.

(6) Avci, C. O.; Garello, K.; Ghosh, A.; Gabureac, M.; Alvarado, S. F.; Gambardella, P. Unidirectional spin Hall magnetoresistance in ferromagnet/normal metal bilayers. *Nat. Phys.* **2015**, *11*, 570−575.

(7) Cubukcu, M.; Boulle, O.; Drouard, M.; Garello, K.; Onur Avci, C.; Mihai Miron, I.; Langer, J.; Ocker, B.; Gambardella, P.; Gaudin, G. Spin-orbit torque magnetization switching of a three-terminal perpendicular magnetic tunnel junction. *Appl. Phys. Lett.* **2014**, *104*, 042406.

(8) Garello, K.; Miron, I. M.; Avci, C. O.; Freimuth, F.; Mokrousov, Y.; Blügel, S.; Auffret, S.; Boulle, O.; Gaudin, G.; Gambardella, P. Symmetry and magnitude of spin-orbit torques in ferromagnetic heterostructures. *Nat. Nanotechnol.* **2013**, *8*, 587−93.

(9) Zhu, L.; Ralph, D. C.; Buhrman, R. A. Spin-Orbit Torques in Heavy-Metal−Ferromagnet Bilayers with Varying Strengths of Interfacial Spin-Orbit Coupling. *Phys. Rev. Lett.* **2019**, *122*, 077201.

(10) Gambardella, P.; Miron, I. M. Current-induced spin-orbit torques. *Philos. Trans. R. Soc., A* **2011**, *369*, 3175−3197.

(11) Avci, C. O.; Quindeau, A.; Pai, C. F.; Mann, M.; Caretta, L.; Tang, A. S.; Onbasli, M. C.; Ross, C. A.; Beach, G. S. Current-induced switching in a magnetic insulator. *Nat. Mater.* **2017**, *16*, 309−314.

(12) Saitoh, E.; Ueda, M.; Miyajima, H.; Tatara, G. Conversion of spin current into charge current at room temperature: Inverse spin-Hall effect. *Appl. Phys. Lett.* **2006**, *88*, 182509.

(13) Avci, C. O.; Beach, G. S.; Gambardella, P. Effects of transition metal spacers on spin-orbit torques, spin Hall magnetoresistance, and magnetic anisotropy of Pt/Co bilayers. *Phys. Rev. B: Condens. Matter Mater. Phys.* **2019**, *100*, 235454.

(14) Razavi, A.; Wu, H.; Shao, Q.; Fang, C.; Dai, B.; Wong, K.; Han, X.; Yu, G.; Wang, K. L. Deterministic Spin−Orbit Torque Switching by a Light-Metal Insertion. *Nano Lett.* **2020**, *20*, 3703−3709.

(15) Bhatti, S.; Sbiaa, R.; Hirohata, A.; Ohno, H.; Fukami, S.; Piramanayagam, S. Spintronics based random access memory: a review. *Mater. Today* **2017**, *20*, 530−548.

(16) Yang, M.; Cai, K.; Ju, H.; Edmonds, K. W.; Yang, G.; Liu, S.; Li, B.; Zhang, B.; Sheng, Y.; Wang, S.; Ji, Y.; Wang, K. Spin-orbit torque in Pt/CoNiCo/Pt symmetric devices. *Sci. Rep.* **2016**, *6*, 20778.

(17) Cai, K.; Yang, M.; Ju, H.; Wang, S.; Ji, Y.; Li, B.; Edmonds, K. W.; Sheng, Y.; Zhang, B.; Zhang, N.; Liu, S.; Zheng, H.; Wang, K. Electric field control of deterministic current-induced magnetization switching in a hybrid ferromagnetic/ferroelectric structure. *Nat. Mater.* **2017**, *16*, 712−716.

(18) Cao, Y.; Sheng, Y.; Edmonds, K. W.; Ji, Y.; Zheng, H.; Wang, K. Deterministic Magnetization Switching Using Lateral Spin−Orbit Torque. *Adv. Mater.* **2020**, *32*, 1907929.

(19) Amin, V. P.; Zemen, J.; Stiles, M. D. Interface-Generated Spin Currents. *Phys. Rev. Lett.* **2018**, *121*, 136805.

(20) Amin, V. P.; Stiles, M. D. Spin transport at interfaces with spin-orbit coupling: Phenomenology. *Phys. Rev. B: Condens. Matter Mater. Phys.* **2016**, *94*, 104420.

(21) Amin, V. P.; Stiles, M. D. Spin transport at interfaces with spin-orbit coupling: Formalism. *Phys. Rev. B: Condens. Matter Mater. Phys.* **2016**, *94*, 104419.

(22) Zhu, L.; Zhu, L.; Shi, S.; Sui, M.; Ralph, D.; Buhrman, R. Enhancing Spin-Orbit Torque by Strong Interfacial Scattering From Ultrathin Insertion Layers. *Phys. Rev. Appl.* **2019**, *11*, 061004.

(23) Fujiwara, K.; Fukuma, Y.; Matsuno, J.; Idzuchi, H.; Niimi, Y.; Otani, Y.; Takagi, H. 5 d iridium oxide as a material for spin-current detection. *Nat. Commun.* **2013**, *4*, 2893.

(24) Kim, J.; Go, D.; Tsai, H.; Jo, D.; Kondou, K.; Lee, H.-W.; Otani, Y. Non-trivial charge-to-spin conversion in ferromagnetic metal/Cu/Al2O3 by orbital transport. *arXiv* **2020**, 2002.00596.

(25) Rojas-Sánchez, J.-C.; Reyren, N.; Laczkowski, P.; Savero, W.; Attané, J.-P.; Deranlot, C.; Jamet, M.; George, J.-M.; Vila, L.; Jaffrès, H. Spin Pumping and Inverse Spin Hall Effect in Platinum: The Essential Role of Spin-Memory Loss at Metallic Interfaces. *Phys. Rev. Lett.* **2014**, *112*, 106602.

(26) Dolui, K.; Nikolić, B. K. Spin-memory loss due to spin-orbit coupling at ferromagnet/heavy-metal interfaces: Ab initio spin-density matrix approach. *Phys. Rev. B: Condens. Matter Mater. Phys.* **2017**, *96*, 220403.

(27) Miron, I. M.; Garello, K.; Gaudin, G.; Zermatten, P.-J.; Costache, M. V.; Auffret, S.; Bandiera, S.; Rodmacq, B.; Schuhl, A.; Gambardella, P. Perpendicular switching of a single ferromagnetic layer induced by in-plane current injection. *Nature* **2011**, *476*, 189−193.

(28) Liu, L.; Pai, C.-F.; Ralph, D. C.; Buhrman, R. A. Magnetic Oscillations Driven by the Spin Hall Effect in 3-Terminal Magnetic Tunnel Junction Devices. *Phys. Rev. Lett.* **2012**, *109*, 186602.

(29) Xie, Q.; Lin, W.; Yang, B.; Shu, X.; Chen, S.; Liu, L.; Yu, X.; Breese, M. B. H.; Zhou, T.; Yang, M.; Zhang, Z.; Wang, S.; Yang, H.; Chai, J.; Han, X.; Chen, J. Giant Enhancements of Perpendicular Magnetic Anisotropy and Spin-Orbit Torque by a MoS2 Layer. *Adv. Mater.* **2019**, *31*, 1900776.

(30) Grigoryan, V. L.; Guo, W.; Bauer, G. E. W.; Xiao, J. Intrinsic magnetoresistance in metal films on ferromagnetic insulators. *Phys. Rev. B: Condens. Matter Mater. Phys.* **2014**, *90*, 161412.

(31) Zhou, L.; Song, H.; Liu, K.; Luan, Z.; Wang, P.; Sun, L.; Jiang, S.; Xiang, H.; Chen, Y.; Du, J.; Ding, H.; Xia, K.; Xiao, J.; Wu, D. Observation of spin-orbit magnetoresistance in metallic thin films on magnetic insulators. *Science Advances* **2018**, *4*, No. eaao3318.

(32) Sinova, J.; Valenzuela, S. O.; Wunderlich, J.; Back, C. H.; Jungwirth, T. Spin Hall effects. *Rev. Mod. Phys.* **2015**, *87*, 1213−1260.

(33) Hoffmann, A. Spin Hall Effects in Metals. *IEEE Trans. Magn.* **2013**, *49*, 5172−5193.

(34) Valet, T.; Fert, A. Classical theory of perpendicular giant magnetoresistance in magnetic multilayers. *J. Magn. Magn. Mater.* **1993**, *121*, 378−382.

(35) Kim, J.; Sinha, J.; Hayashi, M.; Yamanouchi, M.; Fukami, S.; Suzuki, T.; Mitani, S.; Ohno, H. Layer thickness dependence of the current-induced effective field vector in Ta— CoFeB— MgO. *Nat. Mater.* **2013**, *12*, 240−245.

(36) Hayashi, M.; Kim, J.; Yamanouchi, M.; Ohno, H. Quantitative characterization of the spin-orbit torque using harmonic Hall voltage measurements. *Phys. Rev. B: Condens. Matter Mater. Phys.* **2014**, *89*, 144425.

(37) Guerrero, R.; Anadon, A.; Gudin, A.; Diez, J. M.; Olleros-Rodriguez, P.; Muñoz, M.; Miranda, R.; Camarero, J.; Perna, P. Direct determination of Spin-Orbit torque by using dc current-voltage characteristics. *arXiv* **2020**, 2004.02695.

(38) Woo, S.; Mann, M.; Tan, A. J.; Caretta, L.; Beach, G. S. D. Enhanced spin-orbit torques in Pt/Co/Ta heterostructures. *Appl. Phys. Lett.* **2014**, *105*, 212404.

(39) Okabayashi, J.; Koyama, T.; Suzuki, M.; Tsujikawa, M.; Shirai, M.; Chiba, D. Induced perpendicular magnetization in a Cu layer inserted between Co and Pt layers revealed by x-ray magnetic circular dichroism. *Sci. Rep.* **2017**, *7*, 46132.

(40) Garello, K.; Avci, C. O.; Miron, I. M.; Baumgartner, M.; Ghosh, A.; Auffret, S.; Boulle, O.; Gaudin, G.; Gambardella, P. Ultrafast magnetization switching by spin-orbit torques. *Appl. Phys. Lett.* **2014**, *105*, 212402.

(41) Lee, J. W.; Oh, Y. W.; Park, S. Y.; Figueroa, A. I.; Van Der Laan, G.; Go, G.; Lee, K. J.; Park, B. G. Enhanced spin-orbit torque by engineering Pt resistivity in Pt/Co/Al Ox structures. *Phys. Rev. B: Condens. Matter Mater. Phys.* **2017**, *96*, 064405.

(42) Chen, Y.-T.; Takahashi, S.; Nakayama, H.; Althammer, M.; Goennenwein, S. T.; Saitoh, E.; Bauer, G. E. Theory of spin Hall magnetoresistance. *Phys. Rev. B: Condens. Matter Mater. Phys.* **2013**, *87*, 144411.

(43) Chen, Y.-T.; Takahashi, S.; Nakayama, H.; Althammer, M.; Goennenwein, S. T.; Saitoh, E.; Bauer, G. E. Theory of spin Hall magnetoresistance (SMR) and related phenomena. *J. Phys.: Condens. Matter* **2016**, *28*, 103004.

(44) Kim, J.; Sheng, P.; Takahashi, S.; Mitani, S.; Hayashi, M. Spin Hall Magnetoresistance in Metallic Bilayers. *Phys. Rev. Lett.* **2016**, *116*, 097201.

(45) Luan, Z. Z.; Zhou, L. F.; Wang, P.; Zhang, S.; Du, J.; Xiao, J.; Liu, R. H.; Wu, D. Enhanced spin accumulation in metallic bilayers with opposite spin Hall angles. *Phys. Rev. B: Condens. Matter Mater. Phys.* **2019**, *99*, 174406.